

THE HADRONIC τ DECAY OF A HEAVY H^\pm IN ATLAS

KÉTÉVI ADIKLÈ ASSAMAGAN

Hampton University, Hampton, Virginia 23668 USA

AND YANN COADOU

Uppsala University, Uppsala, Sweden

(Received November 21, 2001)

The hadronic τ decay of a heavy charged Higgs boson, $H^\pm \rightarrow \tau\nu$, is considered in ATLAS. In the mass region $m_{H^\pm} > m_t$, the most relevant decay channels of the charged Higgs boson are $H^\pm \rightarrow tb$ and $H^\pm \rightarrow \tau\nu$. Whereas the former suffers from large irreducible backgrounds, the latter offers a relatively clean environment with the appropriate cuts. In addition, a further suppression of the backgrounds is achieved by making use of the polarization of the τ lepton.

PACS numbers: 12.60.Jv, 14.60.Fg, 14.80.Cp

1. Introduction

In the Minimal Supersymmetric Standard Model (MSSM), the Higgs boson sector consists of five physical particles, two of which are charged, H^\pm [1]. Some of the most promising decay channels of the charged Higgs boson have been used to study its discovery potential in ATLAS: below the top-quark mass, the $H^\pm \rightarrow \tau\nu$ has been studied and the signal appears as an excess of τ leptons [2]. The channel $H^\pm \rightarrow Wh^0$ is relevant in a very small area of the MSSM parameter space, thus offering only a marginal discovery potential in ATLAS. However, in the singlet extension to MSSM, *i.e.*, NMSSM, the discovery potential could extend to a more significant range of the parameter space [3, 4]. Above the top-quark mass, the channel $H^\pm \rightarrow tb$ has been studied: discovery is possible for low (< 3) and for high (> 25) $\tan\beta$ up to $m_{H^\pm} \sim 400$ GeV; the diminishing signal rate, in addition to the irreducible backgrounds, prevents the detection of a significant signal in the mass range $m_{H^\pm} > 400$ GeV [5].

The study of the channel $H^\pm \rightarrow \tau\nu$ for $m_{H^\pm} > m_t$ is presented in the current paper. Above the top-quark mass and at high $\tan\beta$, the tb and the $\tau\nu$ channels are the dominant decay channels of the charged Higgs boson while at low $\tan\beta$, the tb is almost exclusively the lone decay channel. Thus, the present study of the $\tau\nu$ channel is carried out in the region $m_{H^\pm} > m_t$ and $\tan\beta > 10$. Unlike the tb decay mode which suffers from large irreducible backgrounds, the $\tau\nu$ channel could be free of such backgrounds, thereby extending the discovery potential beyond that achieved in the tb channel, especially at large $\tan\beta$. Further, an additional suppression of the backgrounds might be possible by taking advantage of the distinctive polarization of the τ lepton.

In the following, we present the details of the current analysis which is carried out in PYTHIA 5.7 [6] — including two-loop radiative corrections to MSSM Higgs boson masses and couplings — and ATLFast [7]. A SUSY spectrum heavier than the charged Higgs boson is assumed with no stop mixing.

2. Analysis

The events are generated in PYTHIA 5.7 using the process $gb \rightarrow tH^\pm$. The associated top quark is required to decay hadronically, $t \rightarrow jjb$. The charged Higgs boson decays into the τ lepton, $H^\pm \rightarrow \tau\nu$, and the hadronic decays of the τ are considered. It is believed that the hadronic decay of the τ carries a better imprint of the τ polarization which can help suppress the backgrounds further [8]. In ATLFast, hadronic τ -jet labelling is performed by requiring hard hadronic τ decay products within the tracking range: $p_T^{\text{had}} > 10$ GeV and $|\eta| < 2.5$; in addition, the hadronic decay products must carry a significant fraction of the τ -jet energy within a jet cone:

$$\frac{p_T^{\text{had}}}{p_T^{\tau\text{-jet}}} > 80\%, \quad (1)$$

$$\Delta R_{(\tau\text{-jet,had})} < 0.1. \quad (2)$$

A τ -jet tagging efficiency of 30% (this corresponds to a jet rejection factor of ~ 400 at $p_T = 30$ GeV [9]) and a b -tagging efficiency of 60% are assumed for an integrated luminosity 30 fb^{-1} . This study assumes a multi-jet trigger in addition to a high level τ trigger. The backgrounds considered are QCD, W +jets, single top production Wtb (derived from ISUB=31 in PYTHIA 5.7), and $t\bar{t}$, with one $W \rightarrow jj$ and the other $W \rightarrow \tau\nu$. The rates for the signal and for the backgrounds are shown in Table I as a function of m_{H^\pm} and $\tan\beta$. The rates for the signal are also shown in Fig. 1 as a function of m_A and for various values of $\tan\beta$.

TABLE I

The expected rates ($\sigma \times \text{BR}$), for the signal $gb \rightarrow tH^\pm$ with $H^\pm \rightarrow \tau\nu$ and $t \rightarrow jjb$, and for the backgrounds: QCD, W+jets, Wtb and $t\bar{t}$ with $t \rightarrow \tau\nu b$ and $\bar{t} \rightarrow jjb$. We assume an inclusive $t\bar{t}$ production cross section of 590 pb. Other cross sections are taken from PYTHIA. The branching fractions of $H^\pm \rightarrow \tau\nu$ are obtained from HDECAY [10], and we take the $W \rightarrow jj$ branching ratio to be 2/3.

Process	$\tan\beta$	m_{H^\pm} (GeV)	$\sigma \times \text{BR}$ (pb)
Signal	20	128	4.81
	18	162	2.54
	15	180	1.33
	30	200	2.23
	40	250	0.91
	45	300	0.54
	25	350	0.10
	35	400	0.13
	60	450	0.23
	50	500	0.11
$t\bar{t}$			84.11
Wtb ($p_T > 30$ GeV)			56.9
W+jets ($p_T > 30$ GeV)			$1.64 \cdot 10^4$
QCD ($p_T > 10$ GeV)			$6.04 \cdot 10^9$

The events are selected as follows (the efficiencies of these selections are shown in Table II):

- (a) Search for one hadronic τ jet with $p_T^\tau > 30$ GeV and $|\eta^\tau| \leq 2.5$, at least three non τ jets with $p_T^{\text{jet}} > 30$ GeV. One of these jets must be a b -tagged jet with $|\eta^b| < 2.5$. Further, we apply a b -jet veto by requiring only a single b -jet with $|\eta| \leq 2.0$ and $p_T > 50$ GeV.
- (b) The W from the associated top quark is reconstructed and the candidates satisfying $|m_{jj} - m_W| \leq 25$ GeV are retained (and their four-momenta are renormalized to the W mass) for the reconstruction of the top quark: this is done by minimizing the variable $\chi^2 = (m_{jjb} - m_t)^2$. We take $m_W = 80.14$ GeV and $m_t = 175$ GeV. Subsequently, the events satisfying $|m_{jjb} - m_t| < 25$ GeV are retained for further analysis. The reconstructions of the W and the associated top quark are shown in Fig. 2.

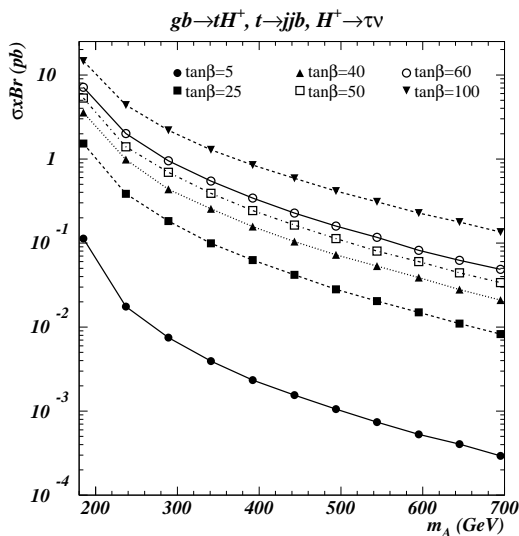


Fig. 1. The rate for the signal as a function of m_A and for different values of $\tan\beta$. The cross sections for the $2 \rightarrow 2$ process, $gb \rightarrow tH^\pm$, are taken from PYTHIA 5.7. The $H^\pm \rightarrow \tau\nu$ branching ratios are obtained from HDECAY. We take the $W \rightarrow jj$ branching fraction to be $2/3$. All the τ decay channels are considered and the hadronic τ decays are selected as described in the text.

- (c) To further reject the backgrounds, we raise the cut on p_T^τ , *i.e.*, $p_T^\tau > 100$ GeV. To satisfy this p_T^τ cut, the τ jet from the backgrounds needs a large p_T boost from the W boson, $W \rightarrow \tau\nu$ [8]. This will result in a smaller opening angle, $\Delta\phi$, between the decay products $\tau\nu$. Here, $\Delta\phi$ is the azimuthal opening angle between the τ jet and the missing transverse momenta. However, in the signal $H^\pm \rightarrow \tau\nu$, the τ jet will require little or no boost at all to satisfy this high p_T^τ cut. This explains the backward peak in the $\Delta\phi$ distribution for the signal as shown in Fig. 3. Similarly, the missing transverse momentum \cancel{p}_T distribution is harder for the signal (see Fig. 2). The transverse mass

$$m_T = \sqrt{2p_T^\tau \cancel{p}_T [1 - \cos(\Delta\phi)]} \quad (3)$$

combines both the effects from the opening angle $\Delta\phi$ and from the transverse missing momentum \cancel{p}_T thereby providing a good discrimination between the signal and the background events as shown in Fig. 3. In addition, the transverse mass m_T is bound from above by m_{H^\pm} for the signal and by m_W for the backgrounds. However, due to the experimental resolution of E_t^{miss} , the m_T distribution for the backgrounds (Fig. 3) shows a “leak” into the signal region.

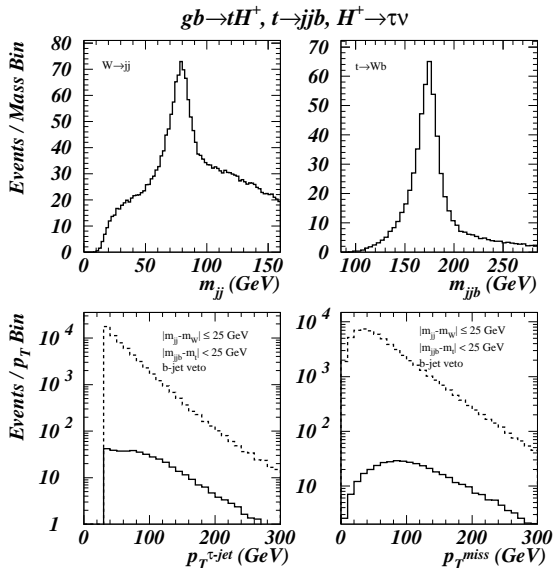


Fig. 2. The mass reconstructions for the W and the top quark (top plots); the p_T^τ and the missing p_T distributions (bottom plots). The data is shown for the signal ($H^\pm \rightarrow \tau\nu$, $m_{H^\pm} = 250$ GeV and $\tan\beta = 40$, solid lines), and for the $t\bar{t}$, W +jets and Wtb backgrounds (dashed lines), for an integrated luminosity of 30 fb^{-1} .

TABLE II

Efficiencies of the cuts (a), (b), (c), (d) and (e) for the signal ($m_{H^\pm} = 250$ GeV, $\tan\beta = 40$) and the backgrounds. Also shown is the successive improvement in the signal-to-background ratios as a result of the cuts. QCD events contribute a negligible background at the cut (d) because of the high threshold imposed on \cancel{p}_T .

Process	(a)	(b)	(c)	(d)	(e)
Signal (%)	19.8	8.7	3.4	1.4	1.1
$t\bar{t}$ (%)	15.6	5.6	0.7	$2.5 \cdot 10^{-2}$	$2.1 \cdot 10^{-3}$
W +jets (%)	$5.0 \cdot 10^{-3}$	$5.6 \cdot 10^{-4}$	$7.0 \cdot 10^{-5}$	$3.0 \cdot 10^{-6}$	$1.0 \cdot 10^{-6}$
QCD (%)	$1.4 \cdot 10^{-4}$	$1.1 \cdot 10^{-5}$	$2.1 \cdot 10^{-7}$	0.0	0.0
Wtb (%)	9.9	2.6	0.19	$6.4 \cdot 10^{-3}$	$1.4 \cdot 10^{-3}$
S/B	$1.9 \cdot 10^{-5}$	$1.1 \cdot 10^{-4}$	$3.6 \cdot 10^{-3}$	0.5	3.4

- (d) To optimize the signal-to-background ratios and the signal significances, we apply a cut on the missing transverse momentum: $\cancel{p}_T > 100$ GeV. Requiring such a high threshold on \cancel{p}_T suppresses completely the QCD jet background as shown in Table II. We cut also on the azimuthal opening angle: $\Delta\phi > 0.5$ rad. The results for the signal and the backgrounds are shown in Fig. 4.

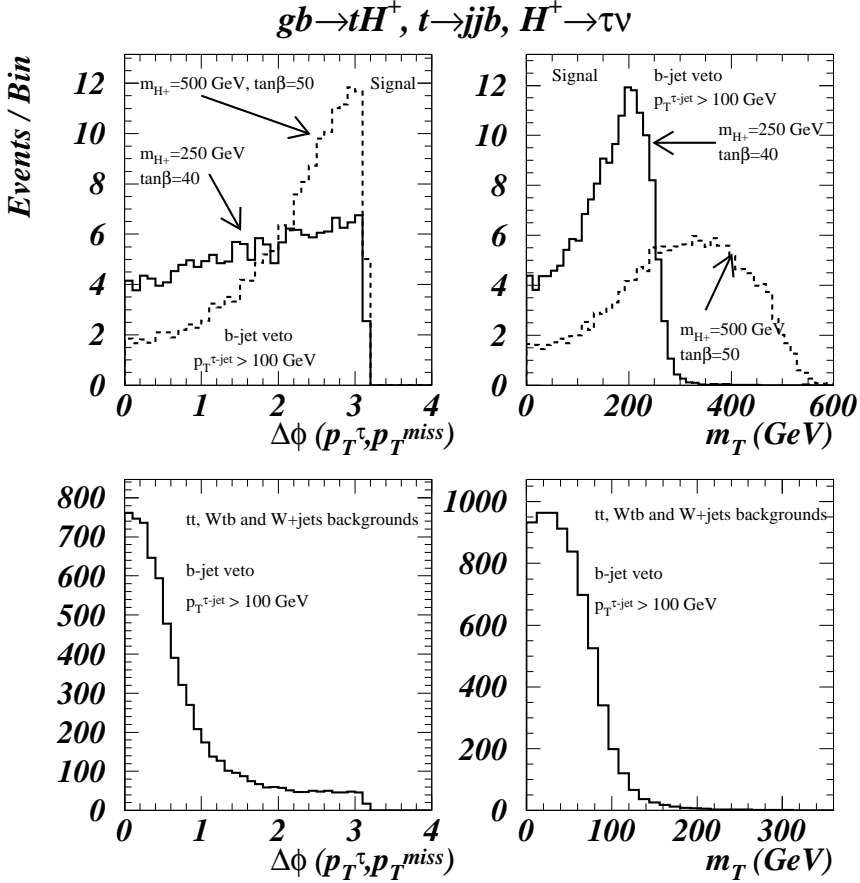


Fig. 3. The opening azimuthal angle $\Delta\phi$ and the transverse mass m_T distributions for the signal (top plots), and for the $t\bar{t}$, Wtb and W +jets backgrounds (bottom plots), for an integrated luminosity of 30 fb^{-1} — obtained after cut (c). The opening angle peaks forward in the backgrounds due to the large boost required from the W boson, while in the signal little or no boost at all is required, and $\Delta\phi$ peaks backward as a result. The transverse mass in the backgrounds is kinematically constrained to be less than m_W but a leak into the signal region can be seen (bottom right plot) due to the experimental E_T^{miss} resolution. In the top plots, the areas of the dashed curves ($m_{H^\pm} = 500 \text{ GeV}$, $\tan\beta = 50$) are normalized to that of the solid curves ($m_{H^\pm} = 250 \text{ GeV}$, $\tan\beta = 40$), with a factor of 4.22.

(e) A final cut of $\Delta\phi > 1.0$ rad is applied and the results are shown in Fig. 5 and used for the calculation of the signal-to-background ratios and the signal significances shown in Table III.

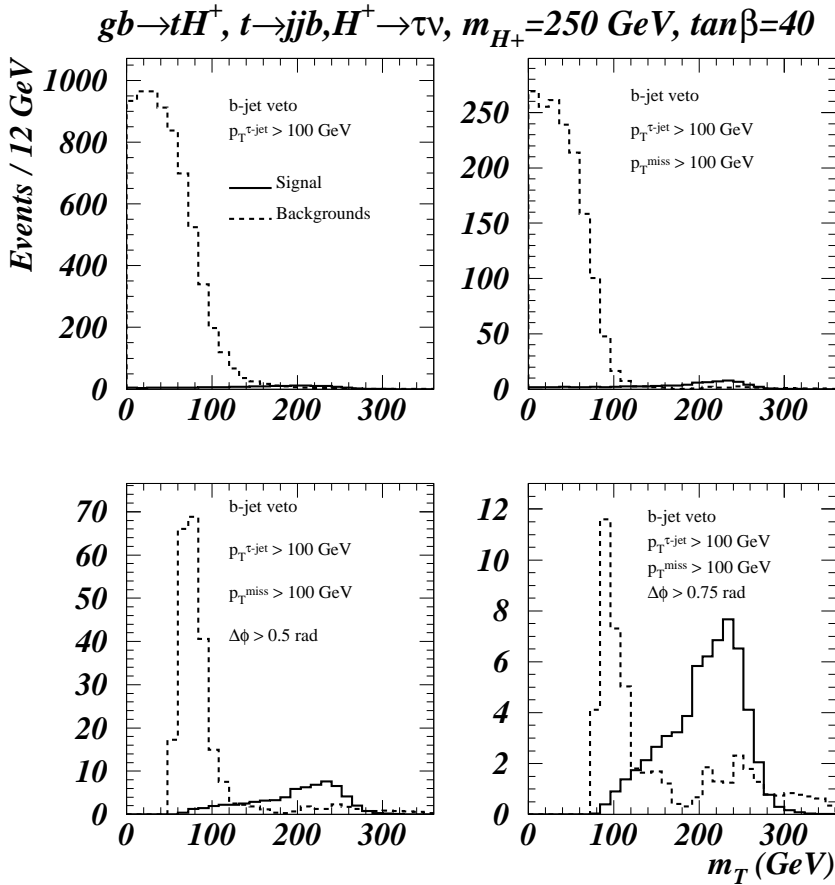


Fig. 4. The transverse mass m_T combines the effects of the $\Delta\phi$ and the differences in the missing p_T distributions for the signal and the backgrounds. Here, we applied further cuts in p_T and in $\Delta\phi$ to optimize the signal-to-background ratios and the signal significances. The top left plot corresponds to cut (c), the top right one to cut (d) but with no selection in $\Delta\phi$. The bottom left plot corresponds to cut (d), and the bottom right plot to cut (d) but with $\Delta\phi > 0.75$ rad.

3. Polarization effects

The polarization of the τ could result in a harder τ jet for the signal relative to the backgrounds in the case of 1-prong decay into π or longitudinal vector mesons; the transverse vector meson contributions dilute the polarization effects and must be eliminated [8, 11, 12]. The transverse contributions could be suppressed without having to identify the individual mesonic con-

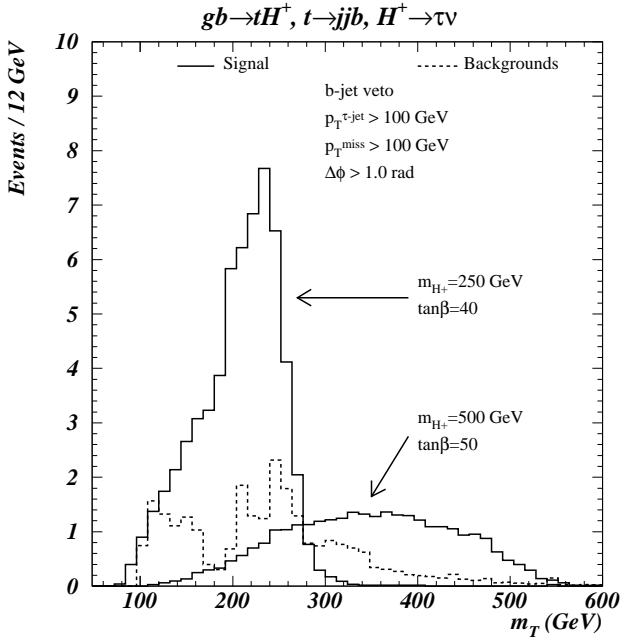


Fig. 5. The transverse mass m_T reconstruction for the signal and the backgrounds for an integrated luminosity of 30 fb^{-1} . The results shown in Table III are based on the data shown here (the unpolarized case), obtained after cut (e) described in the text.

TABLE III

The expected signal-to-background ratios and significances calculated after cut (e) for an integrated luminosity of 30 fb^{-1} . The backgrounds are relatively small; in fact, it is the size of the signal itself that limits the range of the discovery potential.

$\tan \beta$	15	30	40	45	25	35	60	50
m_{H^\pm} (GeV)	180	200	250	300	350	400	450	500
Signal events	9.43	42.7	52.9	61.8	15.9	26.2	51.6	29.1
$t\bar{t}$	10.3	10.3	10.3	10.3	10.3	10.3	10.3	10.3
Wtb	4.24	4.24	4.24	4.24	4.24	4.24	4.24	4.24
W +jets	0.82	0.82	0.82	0.82	0.82	0.82	0.82	0.82
Total background	15.4	15.4	15.4	15.4	15.4	15.4	15.4	15.4
S/B	0.61	2.78	3.44	4.02	1.03	1.71	3.36	1.89
S/\sqrt{B}	2.41	10.9	13.5	15.8	4.05	6.69	13.2	7.41

tributors to the 1-prong decay [8]. One way to do this is to require that over 80% of the τ -jet energy is carried by the charged track,

$$\frac{p_{\pi^\pm}}{p_{\tau\text{-jet}}} > 80\%. \quad (4)$$

Alternatively, one can demand a hard distribution in Δp_T which is the difference in the momenta of the charged track and the accompanying neutral pion(s) [8, 13],

$$\Delta p_T = |p_T^{\pi^\pm} - p_T^{\pi^0}|. \quad (5)$$

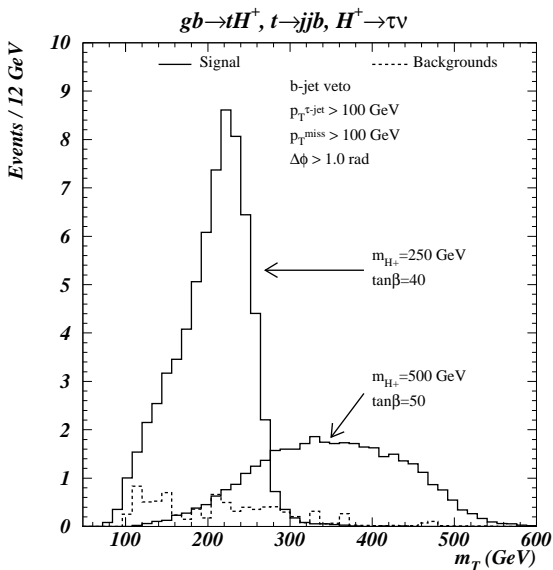


Fig. 6. The final transverse mass m_T reconstruction for the signal and the backgrounds taking into account the polarization of the τ lepton, for an integrated luminosity of 30 fb^{-1} . This is to be compared to Fig. 5, the unpolarized case.

The simulation of the polarized τ decays has been included (for the signal, and the $t\bar{t}$, Wtb and W +jets backgrounds) into PYTHIA through TAUOLA [14], and all the hadronic τ decays have been considered. In Table IV, we show the effect due to the τ polarization. The table shows a reduction in the backgrounds and an enhancement in the signal leading to better signal-to-background ratios and significances but the shapes of the distributions remain similar to that of the unpolarized case (Figs 2-4). The final transverse mass distributions after cut (e) are shown in Fig. 6, to be compared to the unpolarized case of Fig. 5.

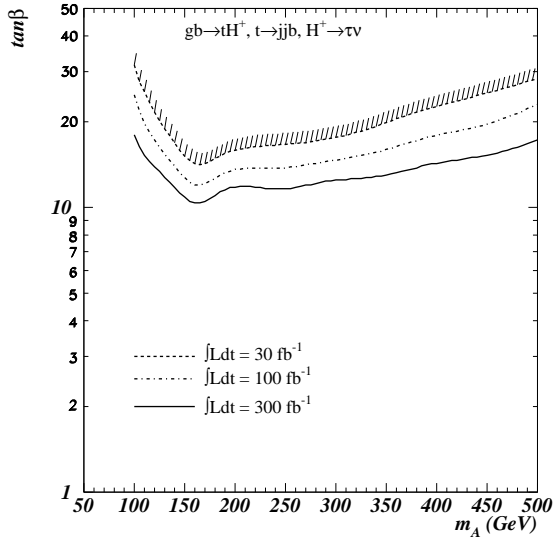


Fig. 7. The 5σ -discovery contour curve in the $(m_A, \tan\beta)$ plane for $gb \rightarrow tH^\pm$ with $H^\pm \rightarrow \tau\nu$ and $t \rightarrow jjb$, for integrated luminosities of 30, 100 and 300 fb^{-1} . The data shown in Table IV and in Table V are used to produce this plot.

We considered two points below the $H^\pm \rightarrow tb$ threshold ($m_{H^\pm} = 180 \text{ GeV}$) and the results are summarized in Table V. These results, together with the data of Table IV, are used to obtain the 5σ -discovery contour of Fig. 7.

We study the effect of the τ polarization further by applying the requirement (4) after the cut (e) defined above. Furthermore, we demand that the charged tracks which satisfy this condition must also pass the following test

$$|\eta^{\pi^\pm}| < 2.5, \quad (6)$$

$$\Delta R_{(\tau\text{-jet}, \pi^\pm)} < 0.1. \quad (7)$$

Henceforth, we refer to these additional cuts as cut (f). If the spectrum contains more than one charged pion, we use the candidate with the highest p_T for the cut (f). Table V shows the results of this cut (f). We note that irrespective of where the requirements (f) are applied in our chain of event selection described in section 2 — see cuts (a)–(e) — they lead to improvements in the signal-to-background ratios and the signal significances, as shown in Table VI, although the number of accepted events is reduced by factors of 3.7 to 22 in both the signal and the backgrounds. Further reductions in the selection efficiencies are expected when one restricts the requirements (f) so as to retain only 1-prong events. Thus, the suppression

TABLE IV

The improvement in the signal to background ratios and signal significances due to the polarization of the τ lepton. The data in this table are calculated after cut (e). We compare the τ decays with and without polarization. The inclusion of the τ polarization suppresses the backgrounds further while at the same time enhances the signal. This results in better signal over background ratios and significances.

	without polarization	with polarization
$t\bar{t}$	10.3	3.1
Wtb	4.2	3.2
W +jets	0.8	0.3
Background events	15.4	6.7
$\tan\beta = 15, m_{H^\pm} = 180 \text{ GeV}$		
Signal events	9.43	13.8
S/B	0.61	2.1
S/\sqrt{B}	2.41	5.3
$\tan\beta = 30, m_{H^\pm} = 200 \text{ GeV}$		
Signal events	42.7	46.3
S/B	2.78	6.9
S/\sqrt{B}	10.9	17.9
$\tan\beta = 40, m_{H^\pm} = 250 \text{ GeV}$		
Signal events	52.9	60.3
S/B	3.44	9.0
S/\sqrt{B}	13.5	23.3
$\tan\beta = 45, m_{H^\pm} = 300 \text{ GeV}$		
Signal events	61.8	70.5
S/B	4.02	10.5
S/\sqrt{B}	15.8	27.2
$\tan\beta = 25, m_{H^\pm} = 350 \text{ GeV}$		
Signal events	15.9	18.8
S/B	1.03	2.8
S/\sqrt{B}	4.05	7.3
$\tan\beta = 35, m_{H^\pm} = 400 \text{ GeV}$		
Signal events	26.2	30.6
S/B	1.71	4.6
S/\sqrt{B}	6.69	11.8
$\tan\beta = 60, m_{H^\pm} = 450 \text{ GeV}$		
Signal events	51.6	66.9
S/B	3.36	10.0
S/\sqrt{B}	13.1	25.8
$\tan\beta = 50, m_{H^\pm} = 500 \text{ GeV}$		
Signal events	29.1	36.2
S/B	1.89	5.4
S/\sqrt{B}	7.42	14.0

TABLE V

The expected signal-to-background ratios and significances calculated after cut (e) for the two points considered below $m_{H^\pm} = 180$ GeV, and for an integrated luminosity of 30 fb^{-1} . This data are also used in the calculation of the 5σ -discovery contour.

$\tan \beta$	20	18
m_{H^\pm} (GeV)	128	162
Signal events	5.3	13.6
Total background	6.7	6.7
S/B	0.8	2.0
S/\sqrt{B}	2.0	5.2

TABLE VI

The implications of the additional cut (f) that we apply to study further the effects of the τ polarization. This cut improves the signal-to-background ratios and the signal significances. However, there are significant drops in the selection efficiencies by factors of 3.7 to 22 in both the signal and the backgrounds, resulting in too few statistics.

	cut (e)	cut (f)
Background events	6.7	0.3
$\tan \beta = 30, m_{H^\pm} = 200 \text{ GeV}$		
Signal events	46.3	12.5
S/B	6.9	48.8
S/\sqrt{B}	17.9	24.6
$\tan \beta = 60, m_{H^\pm} = 450 \text{ GeV}$		
Signal events	66.9	18.3
S/B	10.0	71.5
S/\sqrt{B}	25.8	36.1

of the transverse vector meson contributions to the 1-prong decays results in the enhancement of the signal-to-background ratios and the signal significances but with significant reductions in the selection efficiencies.

4. Conclusions

We have studied the ATLAS discovery potential of the charged Higgs boson through the decay $H^\pm \rightarrow \tau\nu$ above the top-quark mass. For $m_{H^\pm} < m_t$, this channel was previously studied for ATLAS and the signal appears as an excess of τ leptons over SM predictions. In the region $m_{H^\pm} > m_t$, the $\tau\nu$ and the tb decay channels constitute the main decay modes of the charged Higgs boson. At low $\tan \beta$, the tb mode is the only major decay channel of

the charged Higgs boson while at high $\tan\beta$, the branching fraction into the $\tau\nu$ channel can be significant. Previous studies of the tb channel show large irreducible backgrounds which are absent in the $\tau\nu$ channel.

This study is carried out for $m_{H^\pm} > m_t$ and $\tan\beta > 10$. The charged Higgs boson is produced in association with a top quark according to $gb \rightarrow tH^\pm$. We consider the hadronic decay of the associated top quark, $t \rightarrow jjb$ and the hadronic decay of the τ lepton originating from the charged Higgs boson. This study assumes a multi-jet trigger together with a high level τ trigger. By imposing a sufficiently high threshold on the p_T of the τ jet, the background events satisfying this cut need a large boost from the W boson. This results in a small azimuthal opening angle between the τ jet and the missing momentum. In contrast, such a boost is not required from the H^\pm for the signal events, leading to a backward peak in the azimuthal opening angle. Furthermore, the missing momentum is harder for the signal. The difference between signal and background distributions in the azimuthal angle and the missing momentum increases with increasing m_{H^\pm} . These effects are well cumulated in the transverse mass which provides a good discrimination between the signal and the backgrounds — the full invariant mass is not reconstructed in this case because of the neutrino in the final state. For the backgrounds, the transverse mass is kinematically constrained to be smaller than m_W but for the signal, the transverse mass is bound from above by m_{H^\pm} . However, because of the experimental resolution of E_t^{miss} , some leakage of the background events into the signal region is observed. The backgrounds in this channel are relatively small; significances upwards of 5σ can be achieved for $m_{H^\pm} > m_t$ and $\tan\beta > 10$, for an integrated luminosity of 30 fb^{-1} . In fact, the range of discovery potential is solely limited by the signal size itself.

It has been argued that further improvement in the signal-to-background ratios and in the signal significances is still possible by making use of the τ polarization effects. We have included the τ polarization into PYTHIA through the TAUOLA simulation code and considered all the hadronic decays of the τ lepton. Indeed, the present study shows that such an improvement can be statistically significant, and that it is not necessary to restrict oneself to just the 1-prong decays to see the effects of the τ polarization.

The authors express their immense gratitude to E. Richter-Was and R. Kinnunen for fruitful discussions and constructive criticisms. The work of K.A. Assamagan is supported by a grant from the USA National Science Foundation, grant number 9722827.

REFERENCES

- [1] P.H. Nilles, *Phys. Rev.* **110**, 1 (1984); H. Haber, G. Kane, *Phys. Rev.* **115**, 75 (1985).
- [2] D. Cavalli et al., ATLAS Internal Note ATL-PHYS-94-53 (1994).
- [3] M. Dress, M. Guchait, D.P. Roy, hep-ph/9909266; and references therein.
- [4] K.A. Assamagan, ATLAS Internal Note ATL-PHYS-99-025 (1999).
- [5] K.A. Assamagan, ATLAS Internal Note ATL-PHYS-99-013 (1999).
- [6] T. Sjöstrand, “High-Energy Physics Event Generation with PYTHIA 5.7 and JETSET 7.4”, CERN preprints-TH.7111/93 and CERN-TH.7112/93, *Comput. Phys. Commun.* **82** (1994) 74.
- [7] E. Richter-Was, D. Froidevaux, L. Poggioli, ATLAS Internal Note, PHYS-No-079 (1996).
- [8] D.P. Roy, *Phys. Lett.* **B459**, 607 (1999).
- [9] ATLAS Collaboration, ‘ATLAS Detector and Physics Performance Technical Design Report’, CERN/LHCC/99-15, 25 May (1999) 285.
- [10] A. Djouadi, J. Kalinowski, M. Spira, *Comput. Phys. Commun.* **108** (1998) 56.
- [11] B.K. Bullock, H. Hagiwara, A.D. Martin, *Nucl. Phys.* **B395**, (1993) 499.
- [12] S. Raychaudhuri, D.P. Roy, *Phys. Rev.* **D52**, (1995) 1556; **D53**, (1996) 4902.
- [13] R. Kinnunen, “The $H^\pm \rightarrow \tau\nu$ mode in CMS” and “Signatures of Heavy Charged Higgs Bosons at the LHC”, Les Houches Workshop (1999), hep-ph/0002258.
- [14] R. Decker, S. Jadach, M. Jezabek, J.H. Kühn, Z. Was, CERN-TH-6793 (1993), *Comput. Phys. Commun.* **70** (1992) 69, *Comput. Phys. Commun.* **64** (1991) 275, CERN-TH-6195 (1991), CERN-TH-5856 (1990).